Journal of
Composites Science

Article

On the Double-Double Laminate Buckling Optimum for the 18-Panel 'Horse-Shoe' Reference Case

Erik Kappel

German Aerospace Center (DLR), Institute of Lightweight Systems, Lilienthalplatz 7, 38108 Braunschweig, Germany; erik.kappel@dlr.de; Tel.: +49-531-295-2398

Abstract: The Double-Double (DD) laminate family allows for simplification in the context of buckling analysis. Stacking-sequence discussions, known from conventional-laminate optimization, made from 0°, ±45°, 90° plies, omit for DD. The recently presented DD-specific buckling relation is applied in this article to the 18-panel, 'horse-shoe' laminate blending reference case. The use case addresses the challenge of identifying a compatible group of laminates for differently loaded, adjacent regions, as it is a common scenario in wing covers and fuselage skins. The study demonstrates how the novel DD-laminate buckling relation simplifies the process of determining a buckling optimum for a group of laminates. The process of determining the optimum blended DD panel is presented. Its determined mass is compared with minimum masses, presented in earlier studies, which focus on stacking optimization and blending for more conventional ply orientations and laminate stacking conventions.

Keywords: composite design; Double-Double; buckling; optimization; laminate blending; zone-based design

check for updates

Citation: Kappel, E. On the Double-Double Laminate Buckling Optimum for the 18-Panel 'Horse-Shoe' Reference Case. *J. Compos. Sci.* **2024**, *8*, 77. https://doi.org/10.3390/jcs8020077

Academic Editors: Francesco Tornabene and Salvatore Brischetto

Received: 24 November 2023
Revised: 23 January 2024
Accepted: 29 January 2024
Published: 16 February 2024

1. Introduction

Laminate blending denotes the process of defining compatible stacking-sequences for adjacent laminate zones of different thicknesses. 'Compatible' denotes here that a laminate of one zone can be transferred to another zone laminate by dropping a single or a group of plies in order to assure manufacturability. Aerospace parts usually have high-load and moderate-load areas. Figure 1 shows a schematic of a wing. It indicates how selected local loads, due to slats or trailing-edge devices, for example, drive the local laminate thicknesses of the cover.

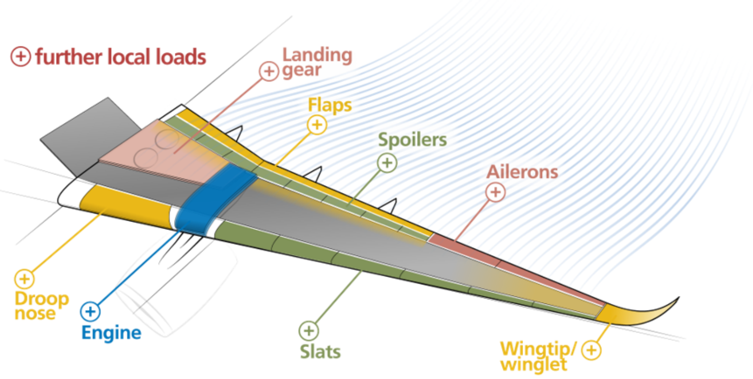

Figure 1. Wing cover schematic—local load introductions drive local laminate thicknesses. Colors indicate selected regions.

The local laminate thicknesses in a cover deviate drastically and considerable effort is mandatory to define zone-to-zone transitions, which meet established laminate design requirements. At the same time, the deduced stacking sequences directly affect the zones' resistance against buckling, which is a critical design driver for thin-walled composite structures. The D_{ij} coefficients of the $[D]$ matrix from the classical laminate theory (CLT) (see Nettles [1]) are stacking-dependent. The D_{ij} are dominant parameters in Equation (1), which describes the buckling of uni- and bi-axially loaded rectangular plates (see [2,3]). The high number of stacking permutations makes the design process challenging, in particular when laminate thickness and the number of plies in the laminate increases. Designers face the following challenges simultaneously:

- Assuring manufacturability ($\rightarrow$ define compatible zone laminates); MDPI: Please check if some contents are missing here.
- Fulfilling the buckling load requirements at the minimum structural weight ($\rightarrow$ identifying the stacking sequence with the highest buckling load within the design space).

Soremekun et al. [4] proposed an 18-panel reference example, which addresses the aforementioned scenario directly. The example addresses the aspects of laminate blending and buckling-load requirements. The reference is also denoted as the 'horse-shoe' use case in the literature. It features 18 individual, simply supported rectangular panels. All panels are subject to bi-axial compression, while no interaction of neighbouring panels is considered.

Figure 2 shows the use case, which is explained in detail in Section 2. Multiple researcher groups [5–13] use Soremekun's example as a reference and provide individual optimal stackings and corresponding minimal masses for blended panels. All those studies focus on more conventional ply orientations, with plies aligned in $[0°, \pm15°, \pm30°, \pm45°, \pm60°, \pm75°, 90°]$, and symmetric laminate architecture (even or odd symmetry).

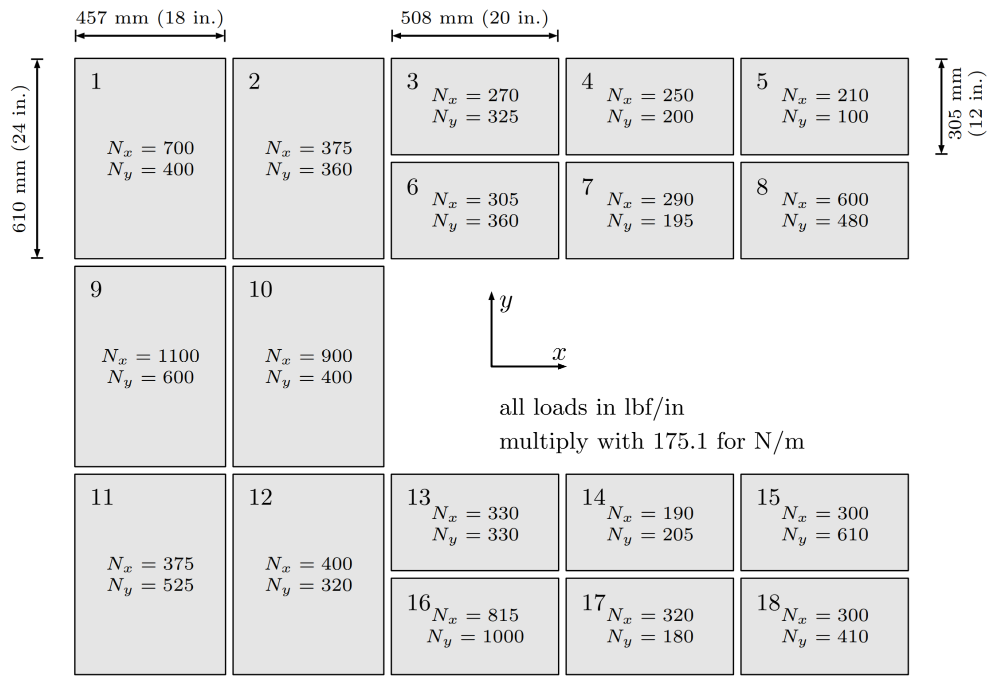

Figure 2. The 18-panel 'horse-shoe' use case. Note that all forces represent compression loads.

The present study adds the first Double-Double solution for Soremekun's example, by applying the results of the recently published article on buckling of simply supported rectangular DD laminates [14].

The present study demonstrates the finding of the DD buckling optimum for the 18-panel reference example. The determination process is outlined and the determined total mass is compared with results presented in earlier studies. Thus, the article quantifies the effect of DD's design-space limitation in terms of structural weight for the first time.

1.1. Buckling of Simply Supported Rectangular Laminates

Buckling of simply supported rectangular composite laminates for uni- and biaxial compression is well described in the literature (see Reddy [2], for example). The Equation

$$N_0(m,n) = \frac{\pi^2}{a^2} \cdot \frac{D_{11}m^4 + 2(D_{12}+2D_{66})m^2n^2\left(\frac{a^2}{b^2}\right) + D_{22}n^4\left(\frac{a^4}{b^4}\right)}{m^2 + k \cdot n^2\left(\frac{a^2}{b^2}\right)} \tag{1}$$

$$= \lambda(m,n) \cdot N_x \quad . \tag{2}$$

describes the relation between the critical buckling load, the panel dimensions and the bending–stiffness properties. The parameter $k = N_y/N_x$ represents a load factor, with $(k = 0)$ being the special case of uni-axial compression in x-direction. The parameters a, b refer to the panel dimensions in the x and y directions, respectively. The D_{ij} refer to ij-coefficient of the bending stiffness matrix $[D]$, which are obtained using classical lamination theory (CLT) (see, for example, [1,15,16]). The parameter $\lambda(m,n)$ is denoted as the buckling factor (see [10], for example), with m, n being the number of half waves along the x and y directions, respectively (see section Appendix A.1 in the Appendix for the definition). The effects of D_{16} and D_{26} are usually assumed to be small (see [4]) or zero (see [9]). This is also adopted for the present article and the assumption is substantiated by the fact that DD's repeat parameter $r \geq 4$ is found as the lower threshold of building block repeats, which further minimizes D_{16} and D_{26}.

1.2. Double-Double Laminate Family Basics

The present article is focused on the family of Double-Double (DD) laminates. A DD laminate is defined by only two individual ply angles φ and Ψ, which are combined (each positive and negative) in a balanced four-ply building block (BB), for example, $[\varphi, -\Psi, -\varphi, \Psi]$. Those BBs are simply stacked on each other, while the laminate symmetry requirement is omitted. The number of BBs is described by the repeat parameter r, leading to an example laminate $[\varphi, -\Psi, -\varphi, \Psi]_{rT}$. The index T denotes 'total', which follows the convention of Nettles [1] and the aforementioned publications in the context of DD. Thickness-normalized descriptions are usually used in the context of DD (see [17,18]). Those are deduced from the CLT's basic relation, as shown hereafter.

$$\underbrace{\begin{pmatrix}\{N\}\\\{M\}\end{pmatrix} = \begin{bmatrix}[A] & [B]\\ [B] & [D]\end{bmatrix} \cdot \begin{pmatrix}\{\varepsilon^0\}\\\{\varkappa\}\end{pmatrix}}_{\text{CLT}} \rightarrow \underbrace{\begin{pmatrix}\{\sigma^0\}\\\{\sigma^f\}\end{pmatrix} = \begin{bmatrix}[A^*] & [B^*]\\ 3[B^*] & [D^*]\end{bmatrix} \cdot \begin{pmatrix}\{\varepsilon^0\}\\\{\varepsilon^f\}\end{pmatrix}}_{\text{Normalized format}} \tag{3}$$

Stresses and strains are $\{\sigma^0\} = \frac{1}{t_{lam}} \cdot \{N\}$, $\{\sigma^f\} = \frac{6}{t_{lam}^2}\{M\}$ and $\{\varepsilon^f\} = \frac{t_{lam}}{2}\{\varkappa\}$. This thickness normalization leads to the fact that all matrices have the same unit, MPa. The publication [14] shows that Equation (1) can be considerably simplified for DD laminates. The normalized bending–stiffness matrix $[D^*]$ plays a key role for the simplification. It is defined as

$$[D] = \frac{t_{lam}^3}{12} \cdot [D^*] = \frac{16 \cdot r^3 \cdot t_{ply}^3}{3} \cdot [D^*] \quad . \tag{4}$$

Reformulating Equation (1) with use of the D_{ij}^* coefficients, leads to

$$N_0(m,n) = r^3 \cdot \frac{16 \cdot t_{ply}^3}{3} \cdot \frac{\pi^2}{a^2} \cdot \frac{D_{11}^*m^4 + 2(D_{12}^*+2D_{66}^*)m^2n^2\left(\frac{a^2}{b^2}\right) + D_{22}^*n^4\left(\frac{a^4}{b^4}\right)}{m^2 + k \cdot n^2\left(\frac{a^2}{b^2}\right)} \quad , \tag{5}$$

which can be solved for the BB repeat parameter r (see section Appendix A.2 in the Appendix for a direct thickness calculation).

$$r = \frac{\sqrt[3]{a^2}}{t_{ply}} \sqrt[3]{N_0(m,n)} \cdot \sqrt[3]{\frac{3}{16\pi^2}} \cdot \sqrt[3]{\frac{m^2 + k \cdot n^2 \left(\frac{a^2}{b^2}\right)}{D^*_{11} m^4 + 2\left(D^*_{12} + 2D^*_{66}\right) m^2 n^2 \left(\frac{a^2}{b^2}\right) + D^*_{22} n^4 \left(\frac{a^4}{b^4}\right)}} \tag{6}$$

While the D_{ij} coefficients in the CLT depend on the specific stacking sequence, it is observed for DD laminates that the considered D^*_{ij} coefficients are independent of r, as the matrix population shows the following scheme.

$$[D^*] = \begin{bmatrix} \cancel{f(r)} & \cancel{f(r)} & \frac{1}{r^2} \cdot (\ldots) \\ \cancel{f(r)} & \cancel{f(r)} & \frac{1}{r^2} \cdot (\ldots) \\ \frac{1}{r^2} \cdot (\ldots) & \frac{1}{r^2} \cdot (\ldots) & \cancel{f(r)} \end{bmatrix} \quad . \tag{7}$$

As a consequence, the term $\sqrt[3]{\frac{m^2 + k \cdot n^2 \left(\frac{a^2}{b^2}\right)}{D^*_{11} m^4 + 2\left(D^*_{12} + 2D^*_{66}\right) m^2 n^2 \left(\frac{a^2}{b^2}\right) + D^*_{22} n^4 \left(\frac{a^4}{b^4}\right)}}$ in Equation (6) is independent from r. It only depends on the half-wave pattern, defined by m and n. As the other factors $\frac{\sqrt[3]{a^2}}{t_{ply}}$ and $\sqrt[3]{\frac{3}{16\pi^2}}$ are constant for a specific panel, one finds the proportionality

$$r \propto \sqrt[3]{N_0} \quad . \tag{8}$$

This remarkable observation changes the whole procedure of laminate optimization for buckling. Determining the minimum laminate thickness is transferred to determining the minimum number of BB repeats. Both are proportional ($t_{lam} = 4 \cdot r \cdot t_{ply}$), but focusing on repeats is more convenient, as the DD laminate concept features full building blocks only.

Identifying the best DD laminate for a certain panel, defined by its dimensions (a, b), a load scenario (defined by N_x and k) and the material-specific ply thickness (t_{ply}), is carried out by executing the following procedure (note that 1° angle-increments for Ψ and φ are considered hereafter): The full DD design space is visualized in Figure 3. Equation (6) is evaluated for each of the 4186 building block combinations, while for each combination multiple, half-wave cases are examined in order to identify the most critical case.

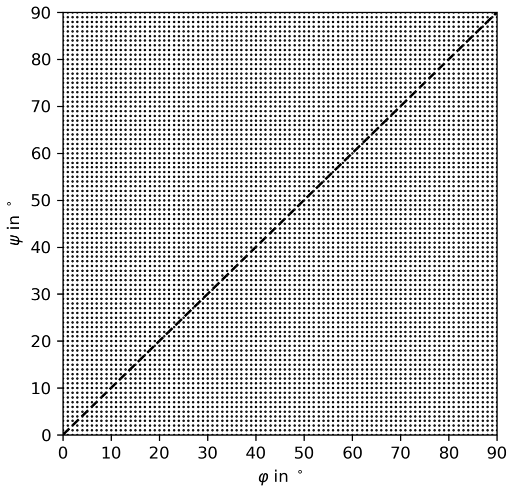

Figure 3. DD design space with $n^2 = 91^2 = 8281$ combinations, which reduce to $n(n+1)/2 = 4186$ combinations due to symmetry.

For an assumed half-wave range of $m = n = [1, 2, 3]$ this leads to nine individual case-specific results for r for each design point. The highest out of those nine r-values is the relevant one, as it directly refers to the most critical buckling case. Equation (6) usually provides a positive real-type number. This does not comply with the integer type of the repeat parameter r, which refers to full four-ply BBs. Thus, the determined real-type r value must be rounded up to the next higher integer to determine the feasible minimum DD laminate thickness.

The outlined procedure is hereafter applied to the 18-panel 'horse-shoe' use case, which has been intensively investigated by multiple researcher groups [4–13], which all focus on blending of conventional, non-DD laminates.

2. The 18-Panel 'Horse-Shoe' Use Case

Figure 2 shows the 'horse-shoe' use case, which consists of 18 rectangular panels. Each panel is considered as simply supported at all four edges. Mechanical panel interaction is not considered. The example consists of panels with the two aspect ratios $a/b = [3/4, 5/3]$. All panels experience bi-axial compression, with the loading parameter $k = N_y/N_x$ being in the range of $k = [0.444, \ldots, 2.033]$. Figure A1 in the Appendix A summarizes additional panel-specific geometrical and load details. All the available studies refer to Hexcel's IM7/8552 unidirectional prepreg [19], which is a carbon fibre epoxy resin material. The relevant prepreg data is provided in Table 1 (note that Seresta et al. [10] provide a density of $\rho = 0.0055$ lb/in^3, which is slightly lower than the value of 0.0057 lb/in^3 provided in the IM7/8552 data sheet [19]).

Table 1. IM7/8552 prepreg. Density of cured ply from data sheet [19].

Property	E_1	E_2	ν_{12}	G_{12}	t_{ply}	ρ
Unit	GPa	GPa		GPa	mm	g/cm^3
Value	141.0	9.03	0.32	4.27	0.191	1.57

Comparisons between the available solutions based on ply count or on the mass M_i of the i-th panel, respectively. The latter is simply calculated based on the panel-specific areas A_i, the local laminate thickness and the material's density ρ.

$$\begin{aligned} M_i &= V_i \cdot \rho \\ &= A_i \cdot t_i \cdot \rho = A_i \cdot n_{ply,i} \cdot t_{ply} \cdot \rho \\ &= A_i \cdot 4 \cdot r_i \cdot t_{ply} \cdot \rho \quad \text{(for DD)} \end{aligned} \tag{9}$$

For studies, in which ply counts are provided only (for example, [8]), the individual panel weights are determined here for the sake of comparability, based on the specific panel areas and the material parameters in Table 1.

Summary of Previous Studies

Soremekun's reference case has been in focus of various studies. Each of those articles provides a stacking optimum, which leads to individual panel masses and the total mass of the blended panel. The present article aims to compare those results with the DD solution presented hereafter in Section 3.

A detailed discussion of the pursued optimization procedures and approaches presented in earlier studies is beyond the scope of the present article. The following comparison utilizes the final results/masses of the available studies only to assess the DD solution, presented in this article. A detailed discussion of the available optimization approaches can be found in Xu et al. [20] and Nikbakt et al. [21].

The individual studies show differences in terms of allowed ply angles and considered laminate stacking rules. Those differences determine the design space and therefore they affect the group of feasible laminate solutions. In the context of panel optimization, more constraints will usually lead to heavier structures. Table 2 provides an overview of the deviating aspects between the studies and outlines the related consequences.

Table 2. Comments of important differences between the available studies.

ID	Comment	Consequence
#1	Ply orientation angles (±) are allowed to vary from 0° to 90° in 15° increments [4–10]	Each ply can have 12 different orientations, which enlarges the design space considerably, compared to laminates used in aerospace practice, which are often composed of 0°, ±45°, 90° plies only. DD also features only four-ply orientations.
#2	Some authors allow for odd ply counts (center-ply symmetry) [4,11], while others enforce even ply counts per panel	This aspect is a potentially disadvantageous aspect for DD laminates, which always feature even ply counts. Moreover, DD ply counts are always multiples of 4 plies, due to the BB architecture. In case a conventional laminate has an optimum at 21 plies, for example, a DD substitute would have 24 plies, leading to an extra mass of 3 plies, when performance equivalence is presumed.
#3	Shvarts and Gubarev [12] consider 0°, ±45°, 90° ply angles only, combined with a set of laminate design guidelines known in practice today, such as stacking symmetry, balance and the 8% orientation-percentages rule, for example	Ply-orientation selection as well as laminate design rules match industry standards. A laminate is composed of only four-ply angles, which is similar to DD.

The laminate constraints considered by Shvarts and Gubarev [12], in particular the limitation to 0°, ±45°, 90° plies combined with both the symmetry and the balance requirement, are close to aerospace standards, such as, for example, shown in context of CFRP frame components [22,23]. In fact, the widely used notation $[\%_{0^\circ}, \%_{\pm 45^\circ}, \%_{90^\circ}]$ represents another indicator for the relevance of the ply orientation selection. A DD laminate basis on only four-ply angles as well. Thus, its design space is smaller compared to the studies presented above [4–10].

All cited studies pursue a comparable general study concept. First, all of the 18 panels are optimized individually, followed by the second analysis step, in which all panel laminates are considered simultaneously. The same procedure is adopted in the present article for the DD case.

Table 3 summarizes the provided panel-weight optima of the previous individual studies. The table focuses on the data of the second analysis step, in which all 18 panels are considered simultaneously, as it refers to the technically relevant scenario of the blended panel.

Table 3. Weight of 18-panel use case provided in previous studies.

Source	Year	Panel Weight	Comments
Soremekun et al. [4]	2002	29.207 kg	Authors presented multiple solutions with identical weight
Adams et al. [5,6]	2004	28.630 kg	
Seresta et al. [10]	2009	28.760 kg	
IJsselmuiden et al. [8]	2009	29.412 kg	
Irisarri et al. [7]	2014	28.799 kg	
Yang et al. [11]	2016	28.910 kg	
Shvarts and Gubarev [12]	2017	31.890 kg	Limited to 0°, ±45°, 90° ply orientation and considering industry stacking rules
Zeng et al. [13]	2019	28.208 kg	Optimum features half ply (=odd laminate ply count for full plies)

One can see that the additional constraints, considered by Shvarts and Gubarev [12], lead to the highest panel mass.

3. DD Application to the 18-Panel Use Case

The set of only three parameters φ, Ψ, r, describe a DD laminate. This allows for a particularly simple illustration of the whole design space. As a similar illustration is not possible for conventional laminates, and therefore quite uncommon, a brief introduction is provided hereafter.

3.1. A Comment on Illustrating DD Results

Figure 4 shows an example. It refers to the distinct load scenario of panel 1, which is presented hereafter.

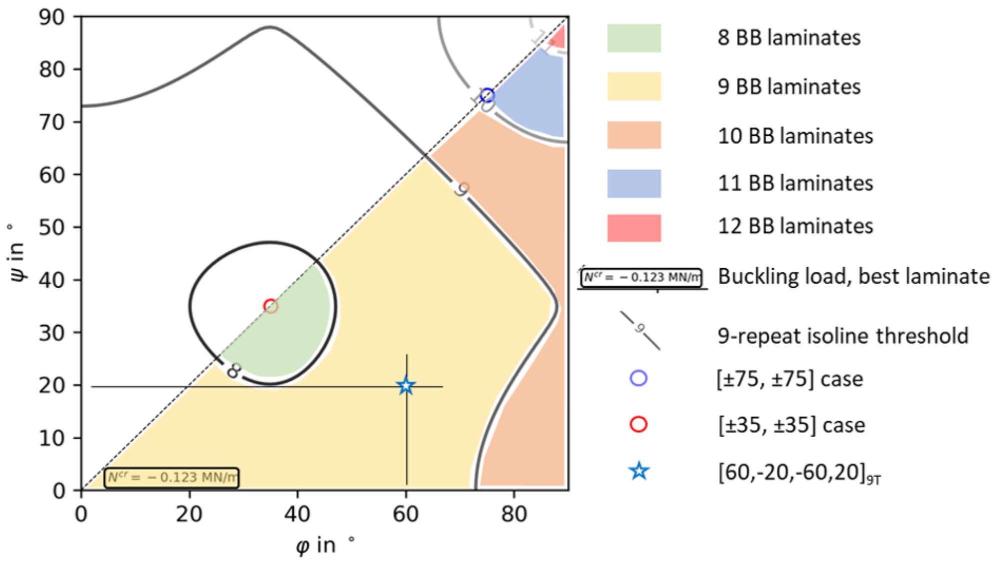

Figure 4. Example graph for panel 1 with highlighted information.

The plot covers the whole design space of conceivable DD laminates for the particular load scenario. Each coloured region refers to a specific number of building block repeats. Thus, a coloured area illustrates laminates of the same thickness and weight. The iso-lines refer to BB repeat thresholds. The yellow region, for example, captures all feasible laminate configurations, which require more than 8 BB but less than 10 repeats. All DD laminates in this region have the same weight. They can sustain the defined load. However, they are four plies thicker than the best laminates, which are indicated by the green region. Laminates close to the iso-line repeated nine times will show smaller load-increase margins than laminates which are close to the threshold repeated eight times.

The plot provides the input buckling load $N^{cr} = N_x$ with $N_y = k \cdot N_x$ in the lower left corner. Figure 5 shows the corresponding graphs for all 18 DD panels. Each plot shows two coloured circles, Those refer to the 18-panel example analysis, which reveals only two individual 'best' BB selections for the group of all 18 panels. For panel 1, $[\pm 35, \pm 35]$ is identified as the best building block. The configuration is located close to the centre of the green-marked region (in Figure 4), which captures all laminates that can sustain the required loads with eight BB repeats. The star in Figure 4 indicates an arbitrary example laminate with a $[60, -20, -60, 20]$ building block. The particular laminate requires nine BB repeats to sustain the defined load of panel 1. The normalized bending stiffness matrix for the star laminate is given by

$$[D^*_{[60,-20,-60,20]_{9T}}] = \begin{bmatrix} 65716.9 & 21537.4 & 240.8 \\ 21537.4 & 48046.1 & 223.2 \\ 240.8 & 223.2 & 22898.7 \end{bmatrix} \mathrm{N/mm^2}. \quad (10)$$

Inserting the D^*_{ij} coefficients in Equation (1) leads to

$$
\begin{aligned}
N_0(m,n) &= 729 \cdot 0.01394\,\text{mm}^3 \cdot 4.726 \cdot 10^{-5} \cdot 1/\text{mm}^2 \\
&\quad \cdot \left(\frac{65716.9 + 2(21537.4 + 2 \cdot 22898.7) \cdot (9/16) + 48046.1 \cdot (81/256)}{1 + 0.571 \cdot (9/16)} \right) \frac{\text{N}}{\text{mm}^2} \\
&= 151.82 \frac{\text{N}}{\text{mm}} \\
&= 1.238 \cdot N_x \quad \rightarrow 23.8\%\ \text{margin, with}\ N_x = \frac{700 \cdot 175.1}{1000} \frac{\text{N}}{\text{mm}}
\end{aligned}
\tag{11}
$$

for the $m = n = 1$ case. The laminate can sustain the panel 1 load case. It shows a 23.8% margin for load increase, which is a consequence of the full building block concept and the related up rounding.

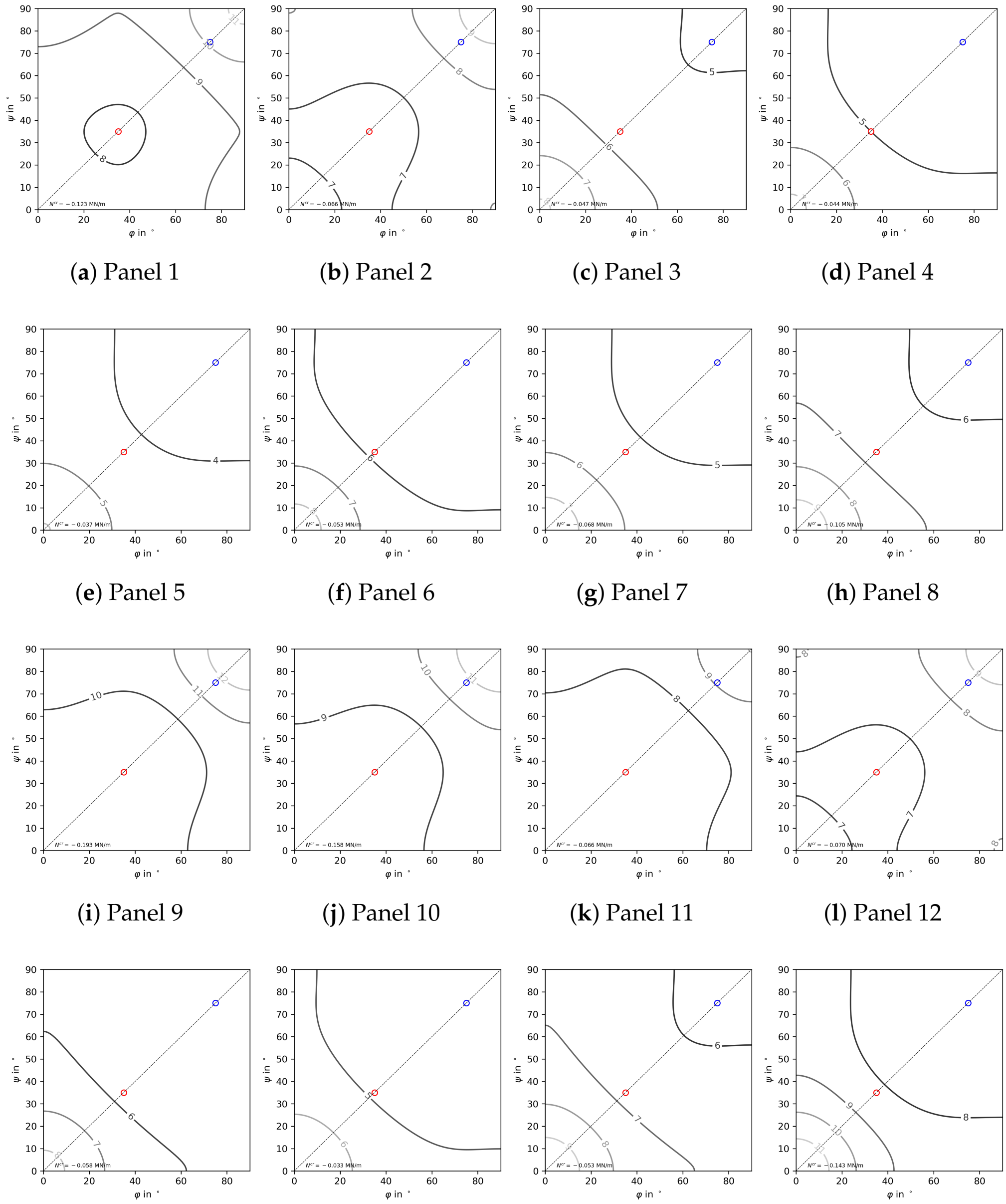

(**a**) Panel 1 (**b**) Panel 2 (**c**) Panel 3 (**d**) Panel 4

(**e**) Panel 5 (**f**) Panel 6 (**g**) Panel 7 (**h**) Panel 8

(**i**) Panel 9 (**j**) Panel 10 (**k**) Panel 11 (**l**) Panel 12

(**m**) Panel 13 (**n**) Panel 14 (**o**) Panel 15 (**p**) Panel 16

Figure 5. *Cont.*

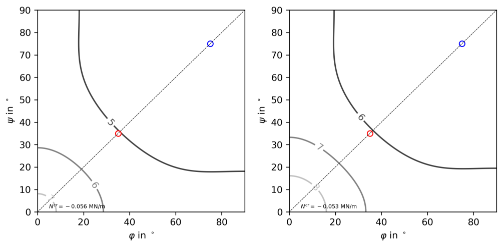

(**q**) Panel 17 (**r**) Panel 18

Figure 5. Minimum-repeat plots for the 18 panels. The red and blue dots refers to [±35, ±35], [±75, ±75] building block angles, respectively.

3.2. The DD 'Horse-Shoe' Results

The DD study comprises the individual analysis of all 18 panels at first, followed by the 'blended' analysis, which simultaneously regards all 18 panels. In both cases the buckling term requirement, from Equation (2), is $\lambda \geq 1$, as in all other studies.

Table 4 summarizes the results of both steps of the study. The first four columns of Table 4 refer to the individual panel analysis. The sum of the individual panel weights is 28.835 kg. The analysis reveals only two different building block optima, with $\varphi = \Psi = 35°$ and $\varphi = \Psi = 75°$. It is found that the identified optimum angles correlate with the panel dimensions. $\varphi = \Psi = 35°$ is obtained for the panels 1, 2, 9, 10, 11 and 12 (all 18″× For all other panels ($a/b = 5/3$) $\varphi = \Psi = 75°$ is obtained. The blended DD panel has a mass of 29.393 kg, which is 2% more than the sum from the individual panel analysis.

Table 4. DD optima—individual panel analysis and blended analysis.

Panel	Individual			Blended			
	Stacking	Total Plies	Weight (kg)	Stacking	Total Plies	Weight (kg)	Margin (%)
1	$[\pm35, \pm35]_{8T}$	32	2.675	$[\pm43, \pm44]_{8T}$	32	2.675	0.0
2	$[\pm35, \pm35]_{7T}$	28	2.341	$[\pm43, \pm44]_{7T}$	28	2.341	7.4
3	$[\pm75, \pm75]_{5T}$	20	0.929	$[\pm43, \pm44]_{6T}$	24 (+4)	1.115	42.3
4	$[\pm75, \pm75]_{5T}$	20	0.929	$[\pm43, \pm44]_{5T}$	20	0.929	19.9
5	$[\pm75, \pm75]_{4T}$	16	0.743	$[\pm43, \pm44]_{4T}$	16	0.743	1.3
6	$[\pm75, \pm75]_{6T}$	24	1.115	$[\pm43, \pm44]_{6T}$	24	1.115	27.9
7	$[\pm75, \pm75]_{5T}$	20	0.929	$[\pm43, \pm44]_{5T}$	20	0.929	3.6
8	$[\pm75, \pm75]_{6T}$	24	1.115	$[\pm43, \pm44]_{7T}$	28 (+4)	1.301	37.0
9	$[\pm35, \pm35]_{10T}$	40	3.344	$[\pm43, \pm44]_{10T}$	40	3.344	25.7
10	$[\pm35, \pm35]_{9T}$	36	3.009	$[\pm43, \pm44]_{9T}$	36	3.009	17.1
11	$[\pm35, \pm35]_{8T}$	32	2.675	$[\pm43, \pm44]_{8T}$	32	2.675	38.1
12	$[\pm35, \pm35]_{7T}$	28	2.341	$[\pm43, \pm44]_{7T}$	28	2.341	6.9
13	$[\pm75, \pm75]_{6T}$	24	1.115	$[\pm43, \pm44]_{6T}$	24	1.115	33.8
14	$[\pm75, \pm75]_{5T}$	20	0.929	$[\pm43, \pm44]_{5T}$	20	0.929	27.1
15	$[\pm75, \pm75]_{6T}$	24	1.115	$[\pm43, \pm44]_{7T}$	28 (+4)	1.301	32.9
16	$[\pm75, \pm75]_{8T}$	32	1.487	$[\pm43, \pm44]_{8T}$	32	1.487	10.1
17	$[\pm75, \pm75]_{5T}$	20	0.929	$[\pm43, \pm44]_{5T}$	20	0.929	17.7
18	$[\pm75, \pm75]_{6T}$	24	1.115	$[\pm43, \pm44]_{6T}$	24	1.115	16.0
			28.835			29.393	

Figure 5 shows the panel-specific minimum-repeats over the DD design space. The aforementioned set of the two optimum solutions $(35°, 75°)$ from the individual analysis is provided in the plots as red and blue circle, respectively.

Figure 6 visualizes the results of the individual panel analysis. Each colour refers to a particular number of repeats.

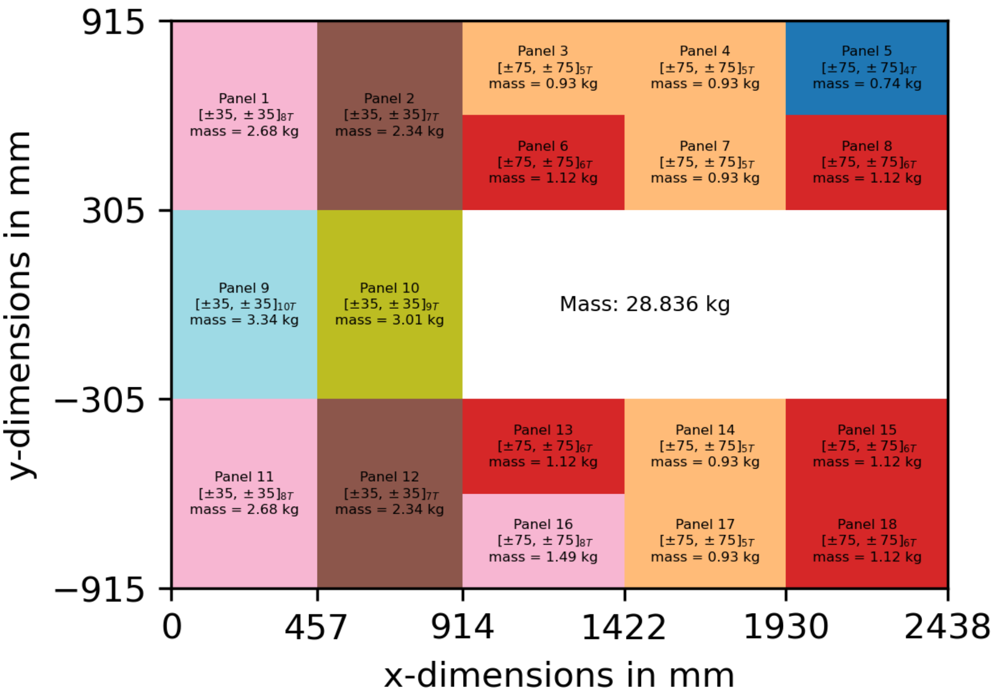

Figure 6. DD results—individual panel analysis. Panel colours refer to particular repeat values.

As different panel-specific optima are obtained, the BB angles for the blended configuration will be 'in-between' the two optima determined from the individual panel analysis. Minimizing the summed mass of all 18 panels was pursued initially to identify the best laminate. The analysis reveals seven solutions in the design space, all with the same total mass of 29.394 kg. Figure 7 shows the seven results as black dots in the centre of the green illustrated 30.0 kg weight region. The green area covers 431 solutions in total with a total mass of ≤30.0 kg.

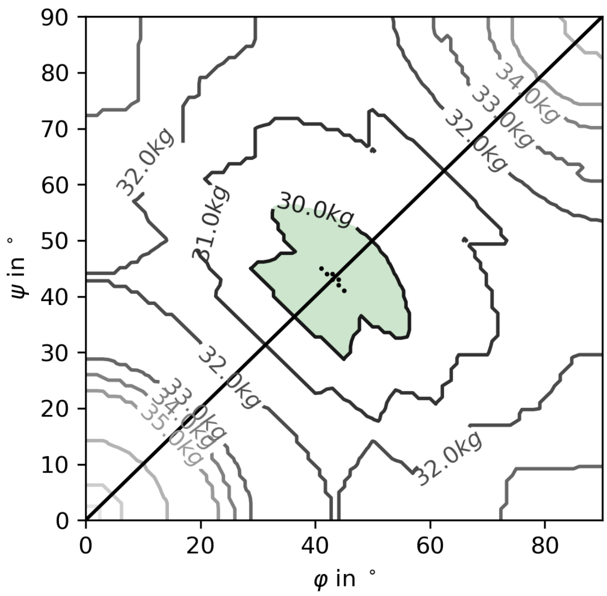

Figure 7. Seven solutions are identified. All lead to the minimum weight of 29.394 kg. The solutions are plotted as black dots in the green region, which covers all laminates below 30.0 kg.

From a weight perspective, all solutions are equivalent. An additional criterion is needed to identify the best solution from the set of seven. Assessing panel-specific load-increase margins can be such an additional criterion. One finds that the summed margins slightly differ for the seven cases, with a maximum for the $[\pm 43, \pm 44]$ building block. Figure 8 shows the corresponding result, with the corresponding margins.

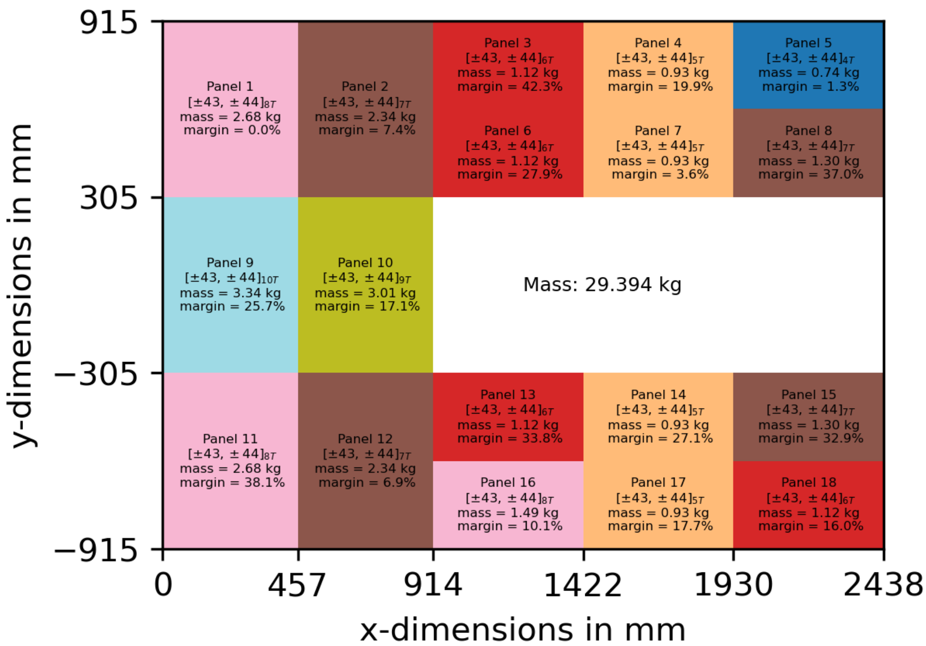

Figure 8. DD combined—selection: Highest total margin, unweighted.

It can be seen that panel 1 is at its load limit, which is indicated by the margin 0.0%. Other panels show higher margins. Thus, panel 1 acts as the driving panel. This observation leads to a potential alternative selection criterion, which focuses on maximizing the margin of the most critical panel 1. Thus, when the solution with the highest margin for panel 1 is selected, the BB $[\pm 43, \pm 43]$ is identified as the best choice, leading to a slightly higher margin of 0.4%. Figure 9 shows the corresponding solution with a focus on the critical panel 1.

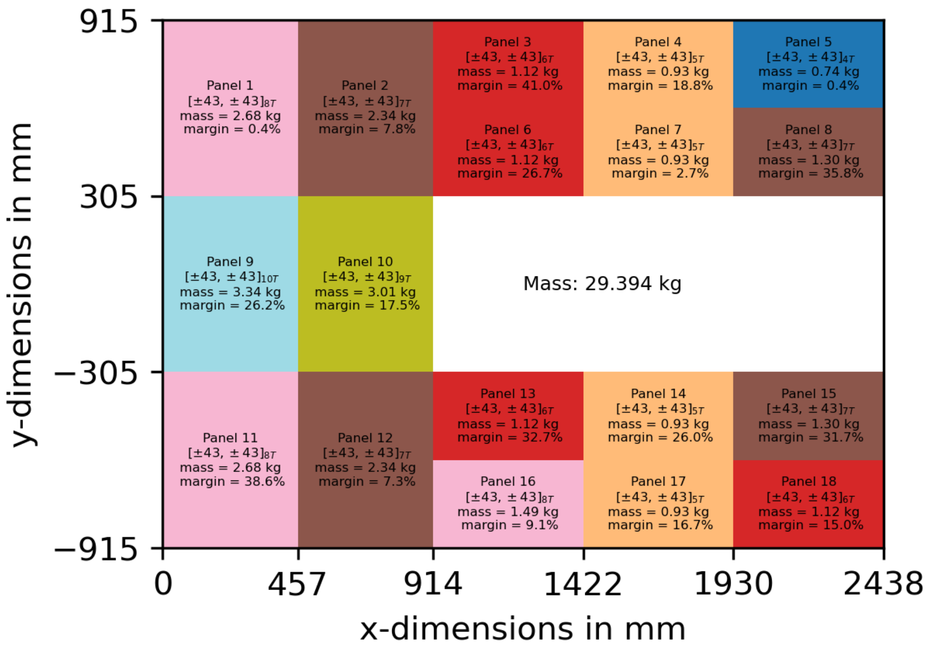

Figure 9. DD combined—angle selection focuses on increasing the margin of panel 1.

However, while the margin of panel 1 is increased, it is found that the specific selection reduces the margin of panel 5, for example, from 1.3% to 0.4%. The final decision requires engineering the judgement and it needs to consider all aspects of the case at hand.

3.3. A Comment on Ply-Angle Increments

As the number of BB repeats is proportional to the laminate thickness, volume and mass, additional plotting options arise. One can directly plot the total mass of all 18 panels over the BB design space, as shown above in Figure 7. The previous DD analysis considers 1° ply angle increments, which is considered a reasonable selection from a manufacturing perspective. Thus, 91 ply angles are covered for φ and Ψ. The weight-iso-lines in Figure 7 show ragged shapes, which are in fact a result of the selected ply angle incrementation. It shall be noted that the 1°-step selection is not a limitation of DD. Finer increments are conceivable. They will lead to smoother iso-lines in the $\Psi - \varphi$ plots, as it has also been shown in [24]. Figure 10 shows the effect of reducing the incrementation from 1° to $1/3^\circ$.

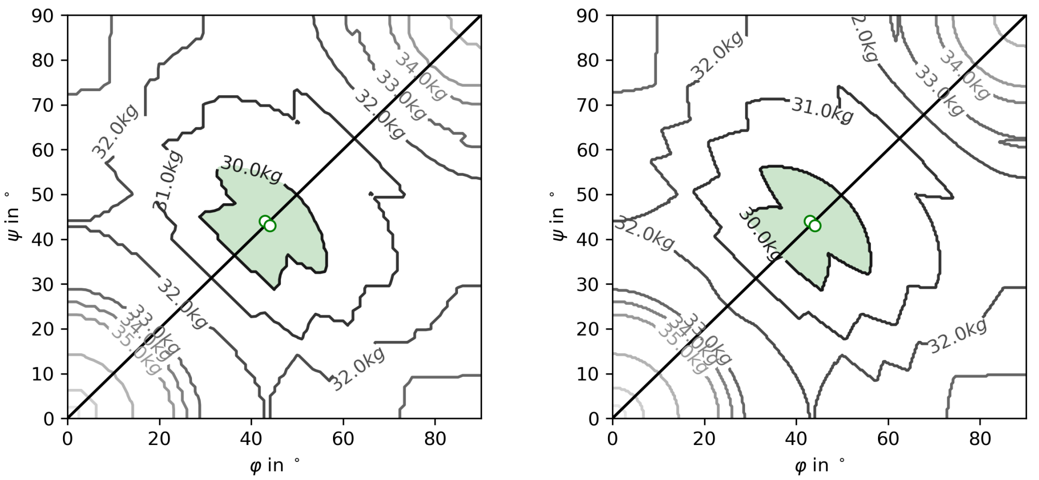

(**a**) 1° resolution (**b**) $1/3^\circ$ resolution

Figure 10. Total weight of all panels over DD design space for different ply angle incrementation.

4. Assessment of DD Results

Table 5 contrasts the DD panel results, presented in Section 3, with the results of the other available studies. The blended optimum DD panel is determined with a weight of 29.394 kg. Other studies provide solutions which are up to 3.8% lighter (-1.1 kg), which suggests a little disadvantage for DD. Even though the direct comparison is straightforward, one must consider that most of the cited studies examine considerably larger design spaces, which allow individual ply orientations $[0^\circ, \pm 15^\circ, \pm 30^\circ, \pm 45^\circ, \pm 60^\circ, \pm 75^\circ, 90^\circ]$. This multitude of ply orientations increases the number of feasible solutions drastically. The large design space is far away from laminates used in industry, which are most often composed of only four discrete ply orientations $[0^\circ, \pm 45^\circ, 90^\circ]$. Thus, it is questionable whether those solutions can act as an industry-relevant reference,

The building block of the DD laminates, in contrast, is defined by only four angles. Thus, the DD laminate design space is remarkably smaller, which is a potential reason for the observed weight penalty.

Shvarts and Gubarev, consider a smaller design space as well. They limit ply orientations to the four angles $[\%0^\circ, \% \pm 45^\circ, \pm 90^\circ]$. The authors further consider constraints such as laminate symmetry and laminate balance, which is considered composite design practice in industry today.

When the result of Shvarts and Gubarev is considered the baseline, the comparison of the DD result reveals a weight advantage of 7.8%, which is equivalent to 2.5 kg for the case at hand.

Table 5. Results at a glance.

Weight	Source	Comment
29.39 kg	**DD configuration**	$[\pm\varphi, \pm\Psi]_{rT}$, full building blocks only, thus total plies always multiples of 4 (22 plies = infeasible)
31.89 kg	Shvarts and Gubarev [12]	Limited to $[0°, \pm45°, 90°]$ plies, considering industrial laminate design rules, as symmetry or 8% rule (among others)
Note: studies hereafter allow a substantially larger design space		
29.21 kg	Soremekun et al. [4]	$[0°, \pm15°, \pm30°, \pm45°, \pm60°, \pm75°, 90°]$ plies are allowed
29.41 kg	IJsselmuiden et al. [8]	Final balanced-blended configuration, $[0°, \pm15°, \pm30°, \pm45°, \pm60°, \pm75°, 90°]$ plies are allowed
28.63 kg	Adams et al. [6]	$[0°, \pm15°, \pm30°, \pm45°, \pm60°, \pm75°, 90°]$ plies are allowed
28.28 kg	Zeng et al. [13]	$[0°, \pm15°, \pm30°, \pm45°, \pm60°, \pm75°, 90°]$ plies are allowed
28.76 kg	Seresta et al. [10]	$[0°, \pm15°, \pm30°, \pm45°, \pm60°, \pm75°, 90°]$ plies are allowed

5. Conclusions

Results of the author's recent work, on buckling of simply supported rectangular Double-Double (DD) laminates, are applied in this article to the 18-panel laminate blending reference use case, which is also denoted as a 'horse-shoe' example. The use case, presented by Soremekun et al. in 2002, is a standard in the context of laminate optimization and laminate blending, which has been examined by multiple research groups in the last two decades. The present article provides a first DD optimum solution for the 'horse-shoe' use case, in order to contrast it with the results of earlier studies.

The determined total mass of the blended DD panel is compared to the optimum masses presented. The blended DD panel offers 7.8% weight reduction, compared to an optimum panel presented by Shvarts and Gubarev, who examined a similar-size design space. Compared to other studies, which examine larger design spaces, the blended DD panel is found up to 3.8% heavier.

Simplicity is a remarkable advantage of DD. While conventional laminate stackings require comprehensive optimization frameworks, to handle millions of conceivable stacking-sequence combinations and their zone-to-zone compatibility in the multi-panel scenario, the best DD solution can directly be determined from a set of analytical calculations. For the 18-panel problem at hand, the set is created in seconds on a conventional desktop PC.

Beyond the panel-weight assessment, the present study demonstrates DD's unique illustration options. The number of BB repeats, the panel masses and also the total mass of the whole 18-panel use case can be plotted over DD's design space, which is defined by only two ply angles φ and Ψ. Similar graphics do not exist for conventional laminates. They are considered valuable for designers in the DD-laminate design process.

Funding: The project '101101974—UP Wing' is supported by the Clean Aviation Joint Undertaking and its members. Funded by the European Union. Views and opinions expressed are however those of the author only and do not necessarily reflect those of the European Union or Clean Aviation Joint Undertaking. Neither the European Union nor the granting authority can be held responsible for them.

Co-funded by the European Union

CLEAN AVIATION

Data Availability Statement: Developed program codes cannot be shared.

Conflicts of Interest: The author declares that he has no known competing financial interests or personal relationships that could have appeared to influence the work reported in this paper.

Abbreviations

The following abbreviations are used in this manuscript:

BB	Building block
CFRP	Carbon-fiber-reinforced plastics
CLT	Classical laminate theory
DD	Double-Double

Appendix A. Panel Facts

Appendix A.1. Margin Definition

Buckling factor definition

$$\begin{aligned}\lambda(m,n) &= \pi^2 \cdot \frac{D_{11}(m/a)^4 + 2(D_{12}+2D_{66})(m/a)^2(n/b)^2 + D_{22}(n/b)^4}{(m/a)^2 N_x + (n/b)^2 N_y} \\ &= \frac{\pi^2}{a^2} \cdot \frac{D_{11}m^4 + 2(D_{12}+2D_{66})(m^2n^2)(a/b)^2 + D_{22}n^4(a/b)^4}{m^2 N_x + n^2(a/b)^2 N_y} \\ &= \frac{\pi^2}{a^2}\frac{1}{N_x} \cdot \frac{D_{11}m^4 + 2(D_{12}+2D_{66})(m^2n^2)(a/b)^2 + D_{22}n^4(a/b)^4}{m^2 + n^2 k(a/b)^2}\end{aligned}$$

leads to: $N_0(m,n) = N_x \cdot \lambda(m,n)$

$$\lambda(m,n) = \frac{N_0(m,n)}{N_x} \tag{A1}$$

Margin is defined as $\lambda - 1$

Appendix A.2. Direct Thickness Calculation

$$\begin{aligned}t_{lam} &= r \cdot 4 \cdot t_{ply} \\ &= \sqrt[3]{a^2}\sqrt[3]{N_0(m,n)} \cdot \sqrt[3]{\frac{12}{\pi^2}} \cdot \sqrt[3]{\frac{m^2 + k \cdot n^2\left(\frac{a^2}{b^2}\right)}{D^*_{11}m^4 + 2\left(D^*_{12}+2D^*_{66}\right)m^2n^2\left(\frac{a^2}{b^2}\right) + D^*_{22}n^4\left(\frac{a^4}{b^4}\right)}}\end{aligned}$$

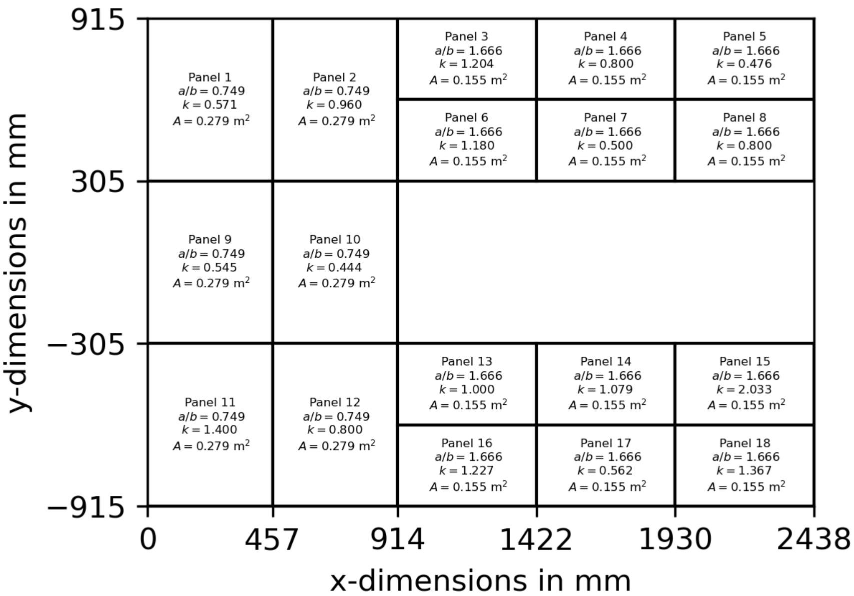

Figure A1. Panel facts.

References

1. Nettles, A.T. *Basic Mechanics of Laminated Composite Plates—NASA Reference Publication 1351*; Technical report; NASA: Washington, DC, USA, 1994.
2. Reddy, J.N. *Mechanics of Laminated Composite Plates and Shells, Theory and Analysis*, 2nd ed.; CRC Press: Boca Raton, FL, USA, 2004.
3. Department of Defense. *Composite Materials Handbook. Polymer Matrix Composites Materials Usage, Design, and Analysis*; MIL-HDBK-17-3F; Department of Defense: Arlington, VA, USA, 2002; Volume 3 of 5.
4. Soremekun, G.; Gürdal, Z.; Kassapoglou, C.; Toni, D. Stacking sequence blending of multiple composite laminates using genetic algorithms. *Compos. Struct.* **2002**, *56*, 53–62. [CrossRef]
5. Adams, D.B.; Watson, L.T.; Gürdal, Z. Optimization and blending of composite laminates using genetic algorithms with migration. *Mech. Adv. Mater. Struct.* **2003**, *10*, 183–203. [CrossRef]
6. Adams, D.B.; Watson, L.T.; Gürdal, Z.; Anderson-Cook, C.M. Genetic algorithm optimization and blending of composite laminates by locally reducing laminate thickness. *Adv. Eng. Softw.* **2004**, *35*, 35–43. [CrossRef]
7. Irisarri, F.X.; Lasseigne, A.; Leroy, F.H.; Le Riche, R. Optimal design of laminated composite structures with ply drops using stacking sequence tables. *Compos. Struct.* **2014**, *107*, 559–569. [CrossRef]
8. IJsselmuiden, S.T.; Abdalla, M.M.; Seresta, O.; Gürdal Z. Multi-step blended stacking sequence design of panel assemblies with buckling constraints. *Compos. Part B* **2009**, *40*, 329–336. [CrossRef]
9. Macquart, T.; Bordogna, M.T.; Lancelot, P.; De Breuker, R. Derivation and application of blending constraints in lamination parameter space for composite optimisation. *Compos. Struct.* **2016**, *15*, 224–235. [CrossRef]
10. Seresta, O.; Abdalla, M.M.; Gürdal, Z. A Genetic Algorithm Based Blending Scheme for Design of Multiple Composite Laminates. In Proceedings of the 50th AIAA/ASME/ASCE/AHS/ASC Structures, Structural Dynamics, and Materials Conference, Palm Springs, CA, USA, 4–7 May 2009.
11. Yang, J.; Song, B.; Zhong, X.; Jin, P. Optimal design of blended composite laminate structures using ply drop sequence. *Compos. Struct.* **2016**, *135*, 30–37. [CrossRef]
12. Shvarts, D.T.; Gubarev, F.V. Towards an Automated Optimization of Laminated Composite Structures. Hierarchical Zoning Approach with Exact Blending Rules. *arXiv* **2017**, arXiv:1705.00819v1.
13. Zeng, J.; Huang, Z.; Chen, Y.; Liu, W.; Chu, S. A simulated annealing approach for optimizing composite structures blended with multiple stacking sequence tables. *Struct. Multidiscip. Optim.* **2019**, *60*, 537–563. [CrossRef]
14. Kappel, E. Buckling of simply supported rectangular Double-Double laminates. *Compos. Part C Open Access* **2023**, *11*, 100364. [CrossRef]
15. Moser, K. *Faser-Kunststoff-Verbund. Entwurfs-und Berechnungsgrundlagen*; VDI Verlag: Düsseldorf, Germany, 1992.
16. Verein Deutscher Ingenieure. *VDI 2014 Blatt 3/Part 3. Development of FRP Components (Fibre reinforced Plastics) Analysis*; Verein Deutscher Ingenieure: Harzgerode, Germany, 2006.
17. Tsai, S.W.; Melo, J.D.D. *Composite Materials Design and Testing—Unlocking Mystery with Invariants*; Stanford University: Stanford, CA, USA, 2015.
18. Tsai, S.W. Double-Double: New Family of Composite Laminates. *AIAA J.* **2021**, *59*, 4293–4305. [CrossRef]
19. HEXCEL. Data Sheet: HexPly 8552 Epoxy Matrix (180 °C/356 °F Curing Matrix). 2013. Available online: https://www.hexcel.com/Resources/DataSheets/Prepreg (accessed on 28 January 2024).
20. Xu, Y.; Zhu, J.; Wu, Z.; Cao, Y.; Zhao, Y.; Zhang, W. A review on the design of laminated composite structures: Constant and variable stiffness design and topology optimization. *Adv. Compos. Hybrid Mater.* **2018**, *1*, 460-477. [CrossRef]
21. Nikbakt, S.; Kamarian, S.; Shakeri, M. A review on optimization of composite structures Part I: Laminated composites. *Compos. Struct.* **2018**, *195*, 158–185. [CrossRef]
22. Garstka, T. Separation of Process Induced Distortions in Curved Composite Laminates. Ph.D. Thesis, University of Bristol, Bristol, UK, 2005.
23. Kappel, E. On abnormal thermal-expansion properties of more orthotropic M21E/IMA carbon-fiber-epoxy laminates. *Compos. Commun.* **2020**, *17*, 129–133. [CrossRef]
24. Kappel, E. Double-Double laminates for aerospace applications—Finding best laminates for given load sets. *Compos. Part C Open Access* **2022**, *8*, 100244. [CrossRef]